Palaeogeography, Palaeoclimatology, Palaeoecology 634 (2024) 111928

Contents lists available at ScienceDirect

Palaeogeography, Palaeoclimatology, Palaeoecology

journal homepage: www.elsevier.com/locate/palaeo

Holocene climate and catchment change inferred from the geochemistry of Lashmars Lagoon, Kangaroo Island (Karti/Karta), southern Australia

Lucinda Cameron Duxbury [a,b,c,d,*], Lluka Yohanni Johns-Mead [a], Haidee Cadd [e], Alexander Francke [a,f], Stefan C. Löhr [a], Wallace Boone Law [g], Linda Armbrecht [c,h], Philip Anthony Hall [a,i], Atun Zawadzki [j], Geraldine E. Jacobsen [j], Patricia S. Gadd [j], David P. Child [j], Charles Maxson [d,k], Zoë Amber Thomas [l,m], Jonathan James Tyler [a,d]

[a] School of Physics, Chemistry and Earth Sciences, Faculty of Sciences, Engineering and Technology, The University of Adelaide, Adelaide, SA 5005, Australia
[b] ARC Centre of Excellence for Australian Biodiversity and Heritage (CABAH), The University of Adelaide, Adelaide, SA 5005, Australia
[c] Australian Centre for Ancient DNA, School of Biological Sciences, The University of Adelaide, Adelaide, SA 5005, Australia
[d] Sprigg Geobiology Centre, The University of Adelaide, Adelaide, SA 5005, Australia
[e] ARC Centre of Excellence for Australian Biodiversity and Heritage (CABAH), University of Wollongong, Wollongong, NSW 2522, Australia
[f] Discipline of Archaeology, College of Humanities, Arts and Social Sciences, Flinders University, Adelaide, SA 5042, Australia
[g] School of Biological Sciences, The University of Adelaide, Adelaide, SA 5005, Australia
[h] Institute for Marine and Antarctic Studies (IMAS), University of Tasmania, Hobart, TAS 7004, Australia
[i] Mawson Analytical Spectrometry Services (MASS), Faculty of Sciences, Engineering and Technology, The University of Adelaide, Adelaide, SA 5005, Australia
[j] Australian Nuclear Science and Technology Organisation (ANSTO), Lucas Heights, NSW 2234, Australia
[k] Department of Geography, Environment, and Population, School of Social Sciences, The University of Adelaide, Adelaide, SA 5005, Australia
[l] School of Geography and Environmental Science, University of Southampton, UK
[m] Chronos ^{14}Carbon-Cycle Facility, University of New South Wales, Australia

ARTICLE INFO

Editor: Dr. Howard Falcon-Lang

Keywords:
Lake sediment
Itrax
X-Ray Diffraction (XRD)
X-Ray Fluorescence (XRF)
Weathering
Hydroclimate

ABSTRACT

We present a continuous ~7000-year sedimentary record from Lashmars Lagoon, Kangaroo Island (Karti/Karta), southern Australia, a region heavily impacted by drought and bushfires in recent decades. Records such as this are vital to contextualise current climatic and environmental shifts, particularly regarding the interplay between hydroclimate and fire-related disturbances in this ecologically sensitive area. We use high-resolution μX-ray fluorescence core scanning, complemented by bulk organic geochemistry and X-ray diffraction mineralogy of catchment soil and lake sediments to reconstruct past climate and catchment processes. Phases of elevated sediment organic matter content (inferred from high Br and total organic carbon) suggest increased lake freshening and productivity, and coincide with increased chemical weathering (inferred from high Al/K and kaolinite/illite and feldspars), likely reflecting the influence of wetter climates. Conversely, periods of high Ca correlate with biogenic carbonate inputs typical of brackish conditions, which we attribute to drier climates or a marine influence. From 7.0 ka, at the mid-Holocene sea level highstand, until 5.7 ka, we suspect Lashmars Lagoon was under virtually continuous influence from the sea. At 5.7 ka, we interpret the abrupt increase in sediment total organic carbon to reflect the severance of the connection to the sea, allowing organic material to accumulate. This, coupled with evidence of high inferred chemical weathering, suggests the climate was relatively wet at the time. After 5.4 ka, our data point to the establishment of drier conditions until the commencement of wetter climates again at 4.5 ka. From 2.5 ka, however, drier climates prevailed again until present. Notably, the climate changes recorded in the sedimentary sequence at Lashmars Lagoon seem to be linked to the strength of the Leeuwin Current, a current that brings warm tropical waters to southern Australia and demonstrates a teleconnection with the El Niño Southern Oscillation, and may well have been an important driver of rainfall on Kangaroo Island (Karti/Karta) over the past ~7000 years.

* Corresponding author at: School of Physics, Chemistry and Earth Sciences, Faculty of Sciences, Engineering and Technology, The University of Adelaide, Adelaide, SA 5005, Australia.
E-mail address: lucinda.duxbury@adelaide.edu.au (L.C. Duxbury).

https://doi.org/10.1016/j.palaeo.2023.111928
Received 15 August 2023; Received in revised form 16 November 2023; Accepted 17 November 2023
Available online 22 November 2023

1. Introduction

Over the coming decades, winter rainfall in southern Australia is predicted to decline, while temperatures, extreme fire danger and droughts are expected to rise – posing a threat to both the environment and the economy (CSIRO and Bureau of Meteorology, 2020; Hennessy et al., 2022). For example, the Millennium Drought – which lasted for about a decade across southeast Australia before ending in 2010 (Van Dijk et al., 2013) – wreaked environmental havoc in the ecosystems of Australia's largest river catchment, the Murray Darling Basin (Bond et al., 2008), and reduced agricultural total factor productivity in Australia by 18% (Sheng and Xu, 2019). More recently, Australia faced its worst recorded bushfire season in 2019–2020 (Davey and Sarre, 2020). The fires claimed 33 human lives, destroyed over 3000 homes, caused immeasurable environmental damage, and resulted in over AU $10 billion of economic losses (Binskin et al., 2020).

To manage and adapt to these changes, it is crucial to understand regional baseline ranges of climatic and environmental variability and adaptability. However, despite the clear need to establish long-term baselines that contextualise current patterns, past climate reconstructions that extend beyond the last century of instrumental observations in Australia are not well constrained. This is due in part to the scarcity of high quality and long-lived palaeoarchives (e.g., tree rings, speleothems, or lake sediments) that record past environmental changes in high temporal resolution – a problem exaggerated in the dry state of South Australia.

Lashmars Lagoon on Kangaroo Island (Karti/Karta,[1] hereby abbreviated to KI; Fig. 1) is a fast-accumulating continuous Holocene sediment record in South Australia (Clark, 1983a). Climate on Kangaroo Island is affected by the El Niño Southern Oscillation (ENSO), which strongly influences eastern Australian climate (Bureau of Meteorology, A., 2022). Further, ENSO has been shown to mediate oceanographic conditions offshore KI such as temperature, salinity and water column stratification, via the Leeuwin Current (LC), on both modern instrumental (Middleton and Bye, 2007) and Holocene (Perner et al., 2018) timescales. The LC is an eastern boundary current, stronger during autumn and winter, that brings warm salty water from the Indo-Pacific Warm Pool down the western coast of Australia and around to just offshore KI (Feng et al., 2003). During El Niño (La Niña) oscillations, when the Indo-Pacific Warm Pool contains less (more) heat, the LC is weaker and cooler (stronger and warmer). The island's climate is also influenced by the position and strength of the Southern Westerly Winds (SWW), which dominate precipitation across the southern portion of the Australian continent (Gillett et al., 2006).

The sediments from Lashmars Lagoon were the focus of pioneering research into past fire and vegetation variability in Australia (Clark, 1983a, 1983b; Singh et al., 1981). These early studies were well-cited in foundational literature that sought to elucidate long term complex interactions between climate, fire, ecosystems and people in Australia (Bowman, 1998; Dodson, 2001; Flannery, 1990; Head, 1989; Horton, 1982; Kershaw et al., 1991; Kershaw et al., 2002; Kohen, 1995; Lampert, 1981; Shulmeister et al., 2004). The original study (Clark, 1983a) presented pollen and microscopic charcoal (microcharcoal) data that revealed (1) a change from *Casuarina* to *Eucalyptus* woodland at ~5 ka – interpreted as a climate drying signal and (2) a marked increase in charcoal concentrations at ~2.5 ka. Clark (1983b) hypothesised this shift might have been caused by the disappearance of people from the island and the subsequent lack of fire management practices. The hypothesis posits that the absence of people would have allowed biomass density to increase, thus leading to bigger fires. Subsequently, analysis of a different core from Lashmars Lagoon used diatom microfossil analysis to infer increasingly saline lake conditions from the mid-Holocene, suggesting that late Holocene aridity may have contributed to cessation of permanent habitation on the island (Illman, 1998). Since its publication, the original record from Lashmars Lagoon has drawn criticism for various reasons (Gammage, 2013; Head, 1989; Illman, 1998). One point of contention relates to the controls on lake salinity at Lashmars Lagoon. The proximity of the lagoon to the ocean and apparent presence of marine gastropods in the sediments suggest that marine incursions may have influenced lake salinity in the past, thus overprinting a climate signal (Clark, 1976). However, the sediment diatom composition has been previously described as dominated by non-marine taxa, implying instead that saline phases were driven by lake evaporation (Illman, 1998).

Now forty years on from the original study, there is an outstanding opportunity to revisit this iconic site with modern techniques providing a high-resolution, multi-proxy record with improved chronological constraint. Critiques and limitations of previous studies emphasise the need to first resolve the depositional history of the sediments and develop a robust chronology. Here, we present a detailed sedimentological study of new core material from Lashmars Lagoon, underpinned by a radiometric chronology that uses a combination of ^{14}C, ^{210}Pb and ^{239}Pu analyses. We combine high-resolution X-ray fluorescence (μXRF) core scanning with mineralogical and organic geochemical analysis of lake and catchment sediment samples to interrogate climate and landscape change over the past ~7000 years. Our findings are then contextualised within broader patterns of regional climate change.

2. Site information

KI is Australia's third largest island, covering an area of 4430 km^2 (Robinson and Armstrong, 1999; Fig. 1). The island was disconnected from the mainland at about 9 ka when rising sea levels severed the land bridge to the mainland (Belperio and Flint, 1999). The island is significant for Aboriginal groups on the adjacent mainland as well as the Tasmanian Aboriginal women who were bought there in the early 1800s, holds historical importance relating to the establishment of the state of South Australia, and is lauded for its unique biodiversity and conservation areas. The climate on KI can be described as dry-temperate, with hot dry summers and mild wet winters (Bureau of Meteorology, 2023).

Lashmars Lagoon is located on the Dudley Peninsula, in the far east of KI (Fig. 1). The Cape Willoughby Lighthouse weather station, 7 km southeast of the lagoon, recorded annual average minimum and maximum temperatures of 13.1 °C and 18.4 °C, and an average annual rainfall of 513.5 mm from 1990 to 2020 (Bureau of Meteorology, 2023). The lagoon is almost permanently wet, although according to locals its surface area and water depth decline significantly in summer (B. Cooter, 2021, personal communication). Occasionally, the lagoon has nearly completely dried out during very dry summers, such as 1914 and 2009. However, even then the surface sediments remained wet in the deepest parts (Clark, 1976) (B. Cooter, 2021, personal communication). When full, the lagoon covers approximately half a square kilometre. In its present state, the lagoon is shallow, brackish (Illman, 1998) and has suffered eutrophication in recent times from the influence of livestock and farming in the area (Environmental Protection Agency, 2013).

The Lashmars Lagoon drains a small catchment area of approximately 60 km^2, the majority of which has been cleared, a process that occurred progressively on the Dudley Peninsula and surrounds since the

[1] Many First Nations groups have strong cultural connections to Kangaroo Island. We have decided to use the Ngarrindjeri word 'Karti' (Gale, 2009) and the Kaurna word 'Karta' (Amery et al., 2021) as alternate names for Kangaroo Island. We do so in an attempt to both maintain a sense of continuity with previous scientific literature (e.g., 'Karta'and 'Kartan', Lampert, 1981) and to reflect what is recorded in modern Aboriginal language dictionaries. This does not reflect an official naming of the island; it is a subjective judgement we have made with publicly available information and limited community consultation. In coming years, we hope to see a conversation to determine an officially recognised dual naming convention for Kangaroo Island from one or more of South Australia's Aboriginal languages.

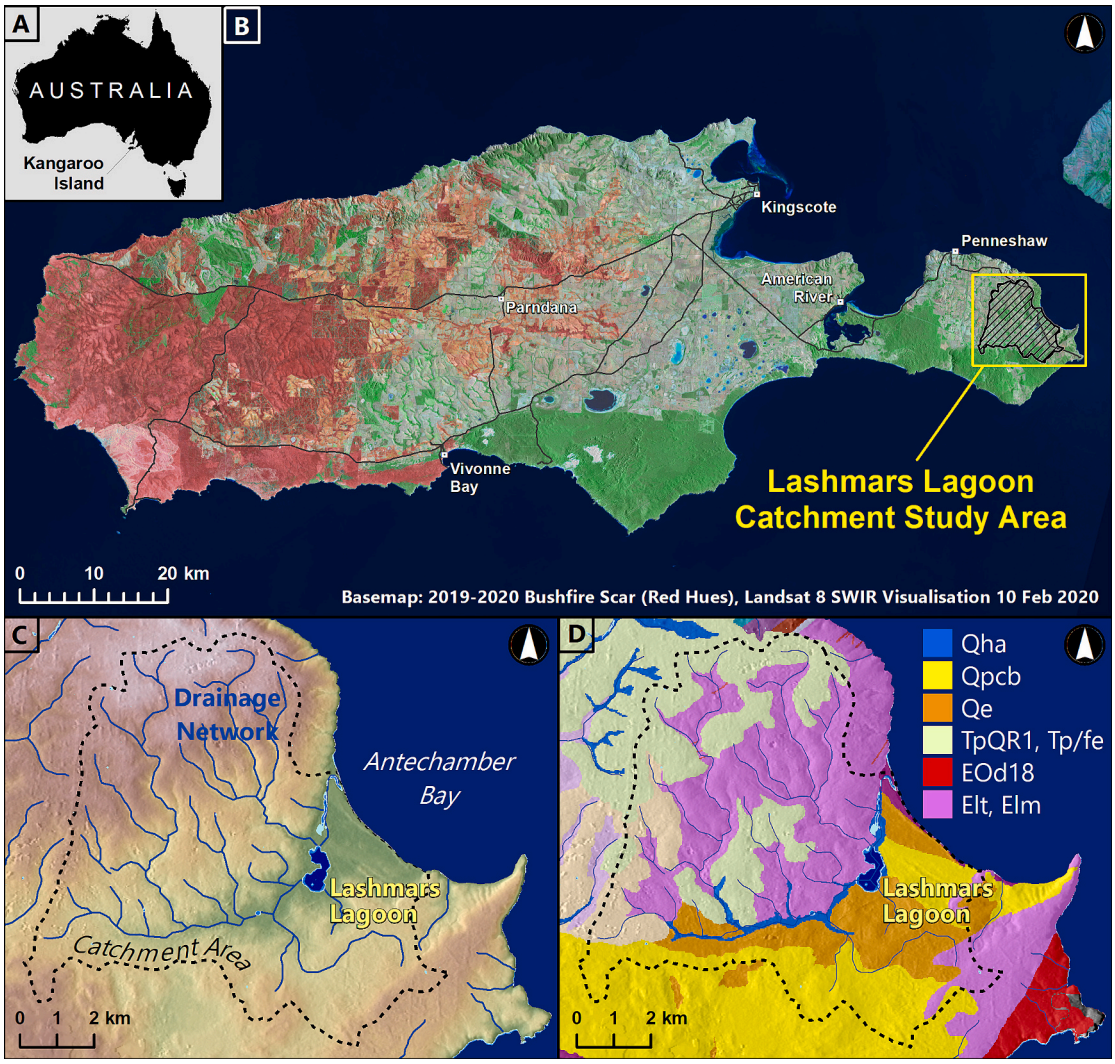

Fig. 1. Map of Kangaroo Island (Karti/Karta) and the Lashmars Lagoon drainage network and catchment. *(A) Kangaroo Island (Karti/Karta) in relation to the Australian mainland. (B) Kangaroo Island (Karti/Karta) overlayed with the fire scar from 2019 to 2020. (C) Lashmars Lagoon catchment and drainage network. (D) Surface geology of the Lashmars Lagoon catchment (sourced from the South Australian Resources Information Gateway (SARIG) online: https://map.sarig.sa.gov.au/). Map units correspond to defined surface geologies: El denotes greywacke to siltstone cycles, sandstone, carbonaceous, sulphidic or calcareous siltstone and shale; EOd4 is Granitoid rock of the Delamerian Orogeny; Qe is aeolian sand of inland dune fields and includes associated alluvial and regolith materials (including calcrete) in interdunal areas; TQr1 or Tp/fe is Early Tertiary to Pleistocene dissected ferruginous duricrust and ferruginous gravel, sand, silt and clay; Qpcb is calcreted aeolianite.*

early 1820s (Taylor, 2008). As of 2013, 60% of the Lashmars catchment was farmland, although the lagoon itself is still fringed by a remnant population of the native South Australian swamp paperbark *Melaleuca halmaturorum* (Environmental Protection Agency, 2013; Clark, 1983a). Three main creeks flow into the lagoon. In order of most to least permanent, they are: (1) a small unnamed creek in the northwest (2) the comparatively large Chapman River in the southwest and (3) an ephemeral winter creek in the southeast (B. Cooter, 2021, personal communication). The lagoon discharges via the downstream Chapman River to the northeast, which reaches the sea after three kilometres at a beach berm that is rarely breached, even after intense rainfall or storms (Clark, 1976). Lashmars Lagoon itself overlays the intersection of three distinct surface geologies (Fig. 1D): (1) Quaternary calcreted aeolianite, (2) Quaternary aeolian sands and (3) interbedded Cambrian greywacke, siltstone, and shale. Early Tertiary to Pleistocene dissected ferruginous duricrust and ferruginous gravel, sand, silt and clay is also present in large swaths in the catchment.

3. Materials and methods

3.1. Sediment coring and field work

Sediment cores were collected from Lashmars Lagoon (Fig. 1; 35.80473°S, 138.06411°E) in September 2020. A ~0.3 m long gravity core (LAS20–1) was collected using a Pylonex HTH corer (Renberg and Hansson, 2008) subsampled in the field at 2.5 mm intervals to recover unconsolidated surface sediments. Using a Bolivia piston corer (Wright, 1967), three proximal discrete holes were drilled in the sediment where the lake was at its deepest (LAS20–2, LAS20–3 and LAS20–4) (Table 1). All cores were stored at 4 °C, in the dark, until further processing at the University of Adelaide, South Australia.

Lake water pH and salinity (PSU) was measured using a HI98194 multiparameter water quality meter (Hanna instruments, Australia). Modern soil and surface sediment samples were collected in November and December 2021 to characterise mineralogical composition. Samples were taken from the lagoon, surrounding catchment, and the streams that flow in and out of the lagoon. These samples were stored at 4 °C until further analysis.

Table 1
Sediment cores retrieved from Lashmars Lagoon, Kangaroo Island (Karti/Karta) in September 2020.

Core name	GPS coordinates (Decimal Degrees)	Coring method	Field depths (cm)	Composite depths (to the nearest cm)
LAS20–1	35.80455°S, 138.06377°E	Gravity corer, extruded at 0.25 cm intervals in the field	Surface – 30 cm	0–30 cm
LAS20–2	35.80481°S, 138.06422°E	65 mm Bolivia corer fitted with 1 m long PVC pipes	0 cm – 400 cm	15–384 cm
LAS20–3	35.80478°S, 138.06418°E		0 cm – 100 cm	19–120 cm
LAS20–4	35.80476°S, 138.06425°E		50 cm – 739 cm	56–749 cm

3.2. Sediment stratigraphy

Bolivia core sections were split lengthways and described for colour, grain-size, structure, consistency, and macrofossil content. Subsequent core correlation was informed by these core log descriptions, complemented by Itrax μXRF data (described below) using the software packages CORRELATOR (cse.umn.edu/csd/correlator) and CORELYZER (cse.umn.edu/csd/corelyzer) according to the workflow set out by Francke et al. (2017) to construct a composite depth scale.

4. Chronology

A total of 26 samples were taken along the composite profile for radiocarbon dating. A total of six plant macrofossils and one shell were picked for dating after visual inspection of the sediments. The plant macrofossils were pre-treated at the Australian Nuclear Science and Technology Organisation (ANTSO), Lucas Heights, using the Acid-Base-Acid method and combusted to form CO_2 using the sealed tube method (Hua et al., 2001). The shell was cleaned by removal of around 10% of the surface using a Dremel® tool followed by chemical etching of further 10% using 0.5 M HCl for 1–5 min under sonication. The shell was treated with 85% H_3PO_4 to evolve CO_2. Carbon dioxide from the macrofossils and the shell was converted to graphite using the H_2/Fe reduction (Hua et al., 2001). AMS ^{14}C measurements on the shell and all macrofossils were carried out using the Vega 1MV accelerator at ANSTO (Wilcken et al., 2015). Pollen concentrates were extracted from 19 bulk sediment samples following Cadd et al. (2022) at the Chronos ^{14}Carbon-Cycle Facility, University of New South Wales. Two ^{14}C measurements were undertaken using a MICADAS (Ionplus, Switzerland) AMS at the Chronos facility (Turney et al., 2021; Wacker et al., 2010), while the remaining 17 samples were analysed at the AMS facility at ANSTO (Wilcken et al., 2015).

A total of 15 samples were dated using ^{210}Pb analysis by alpha spectrometry. Seven samples, each 0.25 cm thick, were taken from the gravity core of the surface sediments at 0 cm, 2 cm, 3 cm, 6 cm, and then at 5 cm intervals from 10 cm to 30 cm. To reach natural background levels of ^{210}Pb concentration, a further eight samples of 1 cm thickness were taken from LAS20-2 at even intervals between 5 and 70 cm from the composite depth profile. To independently validate the ^{210}Pb chronology, 14 one-centimetre-thick samples between 1 and 40 cm were analysed for Pu isotopes. The samples were processed and analysed at the Centre for Accelerator Science, ANSTO (Hotchkis et al., 2019).

The outlier probability of all the radiocarbon dates was calculated using the 'Bchron' package in R (Parnell, 2014). Any date with an outlier probability >0.5 was removed and this process was iterated until all remaining dates had outlier probabilities <0.5. Ages with outlier probabilities <0.5 were then used to construct the age-depth model.

The sedimentary age-depth model for the composite core profile was generated using the *rPlum* package in R which uses Bayesian statistics to combine ^{210}Pb and radiocarbon dates (Aquino-López et al., 2018; Blaauw and Christen, 2011). The model was anchored using the coring date of September 2020 and the 1964 timestamp from the Pu isotopic analysis. Radiocarbon dates were calibrated against the SHCal20 calibration curve (Hogg et al., 2020) and are reported in calibrated years before present (BP), where 'present' is 1950 CE.

4.1. Itrax μXRF core scanning

Sediment cores were scanned on the Itrax μXRF core scanner at ANSTO. All three cores (LAS20–2, −3 and −4) were scanned at 1 mm resolution with a 10 second exposure. LAS20–1, as it was extruded at 2.5 mm intervals in the field, was scanned as discrete dry powdered samples also with a 10 second exposure time.

4.2. Mineralogical analyses

Powder X-ray diffraction (XRD) analysis of 25 samples of ~2 cm^3 from LAS20–4 were conducted at Mawson Analytical Spectrometry Services (University of Adelaide), in addition to 12 catchment samples. Core samples were selected to target significant changes in the Itrax data, as well as to maintain an even spread of samples down core. Where replicates of the same depth were taken, mineralogical proportions were averaged before being included in further analysis.

Samples were freeze dried and crushed using an agate pestle and mortar, and a subset was subsequently micronized. Mineralogy was determined by semi-quantitative XRD analysis using a Bruker D8 ADVANCE Powder X-ray Diffractometer with a Cu-radiation source operating at 40 KV and 40 amps, scanning 2 theta from 5 to 65° with sample rotation of 30 rotations per minute. Data were interpreted using the software package DIFFRAC.EVA (Bruker, Karlsruhe, Germany) and Crystallography Open Database (www.crystallography.net/cod/) reference patterns for identifying mineral phases. Semi-quantitative estimates of mineral composition were obtained by Rietveld modelling using the program DIFFRAC.TOPAS 4.2 (Bruker, Karlsruhe, Germany).

XRD analysis identified gypsum in several samples (see Results). To test whether this gypsum was a primary sedimentary phase or had precipitated when the sample was dried prior to analysis, smear slides of undisturbed wet core material were prepared. Several sand-size grains with morphologies consistent with gypsum were identified in the smear slides. These grains were subsequently analysed using a Bruker Tornado M4 μXRF instrument (25-μm beam, 50 kV/600uA at 20 mbar pressure, 30 s count time). Micro-beam XRF analysis of potential gypsum grains sampled directly from the original wet core material confirmed the gypsum was part of the original sediment composition (Fig. S1).

4.3. Organic geochemistry

Carbon (C) and nitrogen (N) elemental and isotope ratio analyses were performed on 100 mg aliquots of acidified and non-acidified samples, at the Mawson Analytical Spectrometry Services, University of Adelaide. For acidified samples, a 1 g aliquot of each sample was reacted with 2 mL of 10% AnalaR HCl for 20 min to dissolve carbonate, prior to rinsing three times with Milli-Q water. Subsequently, these samples were freeze-dried and reground.

Total C and N for acidified and non-acidified samples were analysed using a Perkin Elmer 2400 series II CHNS/O Elemental Analyser. Samples were analysed in duplicate with results calibrated to the organic analytical standard acetanilide (PerkinElmer, United States). Total Organic Carbon (TOC) of the acidified samples was verified by source rock analysis of the non-acidified samples using a Weatherford Source Rock Analyser. An analysis blank was run with the sample batch and the blank data was automatically subtracted from all analyses. A standard was run at the start of each batch to check instrument status, with additional standards run every 10 samples.

Acidified samples were analysed for $^{13}C/^{12}C$ isotope ratios, reported as $\delta^{13}C_{org}$ (relative to the standard Vienna Pee Dee Belemnite), using a

continuous flow isotope ratio mass spectrometer (Nu Horizon, Wrexham, UK) equipped with an elemental analyser (EA3000, EuroVector, Pavia, Italy). Samples were normalised according to reference values using in-house standards calibrated against USGS and IAEA certified reference materials (USGS40, USGS 41, IAEA-2). Analytical reproducibility was <0.3‰ for all $\delta^{13}C$ analyses.

4.4. Data processing and statistical analysis

Scanning μXRF elemental data was first assessed for low counts per second (cps) at the top and bottom of each core and low cps data were removed. Raw μXRF elemental data were then processed by filtering elements that passed three statistical tests: (1) a runs test to remove elemental data likely affected by non-random artefacts, (2) a percent zero count to remove elemental data comprised of >10% zero values, and (3) a signal to noise ratio test to remove noisy elemental data. We conducted a Pearson's correlation test to compare raw μXRF counts, counts normalised against counts per seconds (cps) and log normalised data. All three normalisation methods were strongly positively correlated with each other (Table S1). For simplicity, we use raw counts per second (cps) for all subsequent analyses.

Principal Components Analysis was performed on the raw elemental data that passed all three tests, to examine the common patterns between elements and identify major determinants of variability in the record. A Pearson's correlation test was used to select elements strongly correlated ($-0.8 > r > 0.8$) with the first two principal component axes (PCs).

Pearson correlation tests were further used to determine statistical correlation between Itrax elemental data, mineralogy, and organic geochemical analyses. Aforementioned data analysis was performed in R version 4.2.0 (R Core Team, 2022). Cluster analysis was applied to the semi-quantitative mineral percentage XRD data from the catchment soil and surface sediment samples using classical cluster multivariate analysis in the software PAST 4.03 (Hammer et al., 2001).

5. Results

5.1. Modern lake parameters

At the time of coring (September 2020), Lashmars Lagoon was brackish (7.40 partial salinity units; 12,790 μmS/cm conductivity) and alkaline (pH 9.9). A coarse survey suggested a maximum water depth of ~90 cm.

5.2. Sediment lithology and chronology

The Lashmars Lagoon sediment cores consist of mainly homogenous, fine grained, organic and clay rich sediments that ranged in colour from greys and black to browns and olives (Fig. 2B). We found no visual indications of hiatuses or erosional surfaces.

Radiocarbon analysis on samples from LAS20–3 and LAS20–4 (94 cm to 728 cm in the composite depth profile) generally displayed a pattern

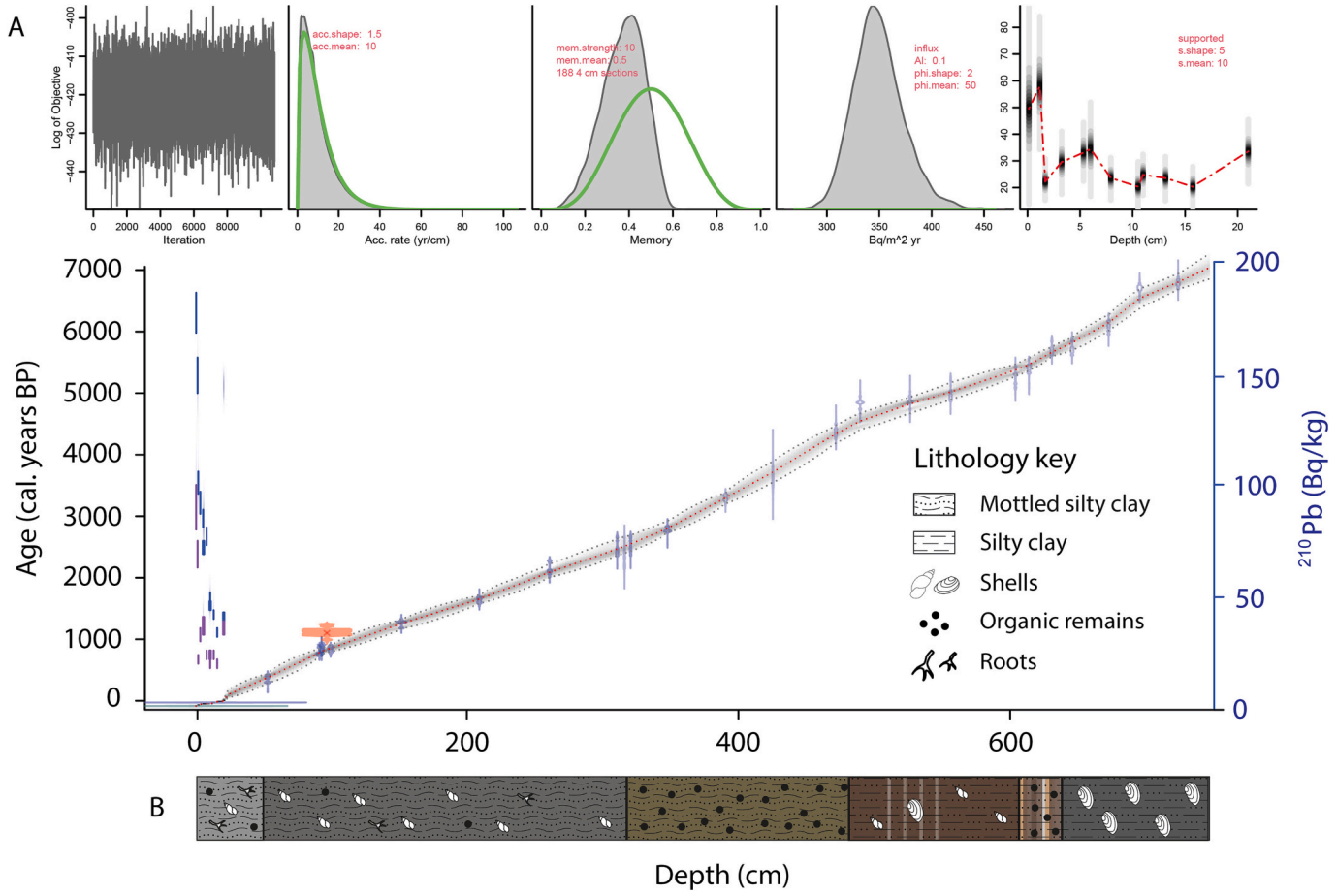

Fig. 2. Age model and lithology of the Lashmars Lagoon sediments. *(A) Bayesian age depth model for the complete 749 cm core, constructed using the package rplum in R. Outliers excluded from the model are denoted in red. The model incorporates radiocarbon and ^{210}Pb dating. The section of the model that relies on ^{210}Pb dating (0–60 cm) is displayed in Fig. S2. The model is anchored with the coring date (September 2020) at 0 cm and the Pu-isotope inferred bomb peak at 1964 at 13.5 cm. (B) Sediment lithology based on visual core description and refined using the XRF data (see Fig. 5 and Table 2 below for more detail). Colour reflects colour of sediments.* (For interpretation of the references to colour in this figure legend, the reader is referred to the web version of this article.)

of increasing age with increasing depth (Fig. 2A). ^{210}Pb measurements from the upper sediments returned unsupported ^{210}Pb concentrations that decreased with depth (Fig. S3). Pu isotopic profiling indicates that the 1964 bomb peak occurred in our sediments at 13.5 cm in the composite depth profile (Fig. S4).

The Bayesian *rplum* model, combining all three dating methods, returned a modelled basal age range of 6840–7230 cal. years BP (mean 7010 cal. years BP) at 749 cm (Fig. 2A). Only one radiocarbon age, the age from the unidentified shell at 97 cm (OZAE54) was offset by ~300 ^{14}C years from its paired macrofossil data, consistent with a reservoir effect, and was excluded from this model with an outlier probability of 96%. All other dates had outlier probabilities <5% in the final iteration. The deepest three ^{210}Pb samples (X324, X325 and X326) were also excluded from the age model as background ^{210}Pb levels had already been reached.

The calculated sediment accumulation rate averaged 1.2 mm/year across the entire record and varied with changes in sedimentology. The accumulation rate is highest in the first 20 cm, corresponding to the early to mid-twentieth century until present day.

5.3. Lake sediment and catchment mineralogy

We used powder XRD analysis to identify fifteen minerals in the sediments of Lashmars Lagoon and surrounding catchment and streams: aragonite, calcite, magnesium calcite, kutnohorite, halite, gypsum, pyrite, biotite, muscovite, illite, kaolinite, quartz, oligoclase, microcline and rutile. For simplicity, we combined the carbonates (calcite, aragonite, magnesium calcite and kutnohorite), the micas (biotite and muscovite) and the feldspars (oligoclase and microcline).

The lake sediments are comprised of varying concentrations of (1) illite, (2) kaolinite, (3) quartz, (4) carbonates, (5) halite, (6) pyrite, (7) feldspars, (8) micas and (9) gypsum (Fig. S4). In general, the inorganic portion of the lake sediment is clay-rich, with illite and kaolinite composing on average ~ 55% of each sample. Quartz and carbonates were also commonly detected in moderate relative abundance in the lake sediments.

We compared the mineralogy of the lake sediments to catchment soils and inflow sediments to better understand the sources of sediment to the lake, and how this might have changed historically (Fig. 3). Cluster analysis (Fig. 4) showed that the modern surface sediments of Lashmars Lagoon are most similar to the Chapman River floodplain sample (b) and the upstream Chapman River samples (g and h). This is consistent with the Chapman River being an important contemporary sediment source to Lashmars Lagoon (Fig. 4A). The Chapman River downstream sediment (a), however, was the most different from, and formed its own sister clade to, the other samples. This likely reflects the addition of authigenic phases from the lagoon, and perhaps highlights inefficient routing of detrital sediments through the lake where this material is trapped. We also considered the relationship between the catchment samples and the downcore sediment samples, evaluating whether the source of sediment to Lashmars Lagoon has changed over time (Fig. 4B). We found a similar pattern of relatedness to the surface sediments: only the upstream Chapman River sediments and floodplain sample cluster with the Lashmars Lagoon sediment samples, suggesting that the source of sediments to Lashmars Lagoon has not changed significantly for much of the past ~7000 years.

5.4. Organic geochemistry

Total Organic Carbon (TOC), total organic carbon to nitrogen (C/N) and δ^{13}C isotopic ratios offer insights into changes in organic matter provenance over time (Meyers and Lallier-Vergès, 1999). TOC values were variable throughout the record, ranging from 3.3 to 13.5%, suggesting notable changes in the catchment and or climate around Lashmars Lagoon over the past ~7000 years (Fig. 6). C/N values ranged from 10.79 to 15.10 and were relatively stable throughout the record except for two comparatively low values of 10.79 and 11.64 at 5.06 ka and 4.27 ka respectively (Fig. S5). These values fall between those typical for algae and terrestrial plants, thus indicating mixed sources of sediment organic matter at Lashmars Lagoon (Meyers, 1994). δ^{13}C values, which can be used to infer photosynthetic processes in plants and algae (e.g., Heyng et al., 2012), were between −21.71 and − 25.44‰ and are relatively low in the sediments older than 3.60 ka and relatively high after this point (Fig. S5).

5.5. Elemental geochemistry

The filtered scanning μXRF data returned 32 detectable elements of the initial 40 captured in the raw data. The first three principal component (PC) axes of the analysis of all 32 elements explained 52.6% of the overall variance (31.5%, 15.6% and 5.2% respectively). We found eight elements strongly correlated with the first two PCs: bromine (Br), calcium (Ca), strontium (Sr), antimony (Sb), potassium (K), titanium (Ti), iron (Fe) and rubidium (Rb) (Table S2). Br and the group of lithic elements containing K, Ti, Rb and Fe were anticorrelated and together explained most of the variation along PC1 (Fig. 5). The elements Ca, Sr and Sb were strongly correlated with PC axis 2. The downcore variation in these key elements is summarised visually in Fig. 6.

Six distinct stratigraphic units were identified from μXRF elements, visual core analysis and sediment accumulation rate: unit 1 (2020 CE – 0.33 ka), unit 2 (0.33–2.53 ka), unit 3 (2.53–4.47 ka), unit 4 (4.47–5.40 ka), unit 5 (5.40–5.72 ka), and unit 6 (5.72–7.01 ka) (Table 2).

Br shows considerable variation throughout the core (Fig. 6); low Br counts were measured in the oldest part of the core from 7.01 to 5.72 ka (unit 6), a brief period of high counts until 5.40 ka (unit 5), an extended low period again until 4.47 ka (unit 4), an extended high period across the middle of the record until 2.53 ka (unit 3), another long low period until 0.33 ka (unit 2) and finally a recent relatively high period until modern day (unit 1). Br correlated strongly with TOC ($r = 0.91$, $p = 0.0006$), consistent with previous work indicating that Br can be a proxy for TOC (Seki et al., 2019; Ziegler et al., 2008). Br also showed a significant positive relationship with halite ($r = 0.92$, $p = 2E\text{-}10$) and kaolinite ($r = 0.66$, $p = 0.0005$).

The group containing the elements K, Ti, Fe and Rb demonstrates an inverse pattern to Br through time (Fig. 6). K and Rb are likely hosted by illite and feldspars, Ti in detrital silicates (e.g., quartz) and rutile, and Fe in oxyhydroxides. This group showed significant positive correlations with the concentration of quartz (e.g., for Rb $r = 0.54$, $p = 0.006$), feldspars (e.g., for Rb $r = 0.67$, $p = 0.0003$) and the sum of quartz, feldspar and illite (e.g., for Rb $r = 0.75$, $p = 0.0001$).

Ca, Sr, and Sb varied considerably through the core, following a somewhat similar trend to the group containing K, Ti, Fe and Rb (Fig. 6). There are moderate to high counts of Ca, Sr, and Sb from 7.01 to 4.47 ka (units 6–4), followed by a phase of very low counts in the middle of the record from 4.47 to 2.53 ka (unit 3), and finally, a period of high counts from 2.53 ka to present day (units 1–2). This group were all positively and significantly correlated with the carbonates (e.g., for Ca $r = 0.68$, $p = 0.0005$). Ca and Sr can also be contained in the evaporite gypsum. When the relative abundances of gypsum and the carbonates were added together, the correlation with the Ca and Sr improved (e.g., for Ca $r = 0.80$, $p = 0.0001$).

In addition to the significant μXRF elements, we considered the elemental ratio Al/K (Fig. 6), which has been used to shed light on chemical weathering and hydroclimate (Burnett et al., 2011; Wei et al., 2006). The Al/K elemental ratio follows the same trends as Br ($r = 0.88$, $p = 0.0001$) and is positively and significantly correlated with the ratio of the Al bearing clay kaolinite to the Al and K bearing minerals illite and feldspars ($r = 0.60$, $p = 0.003$).

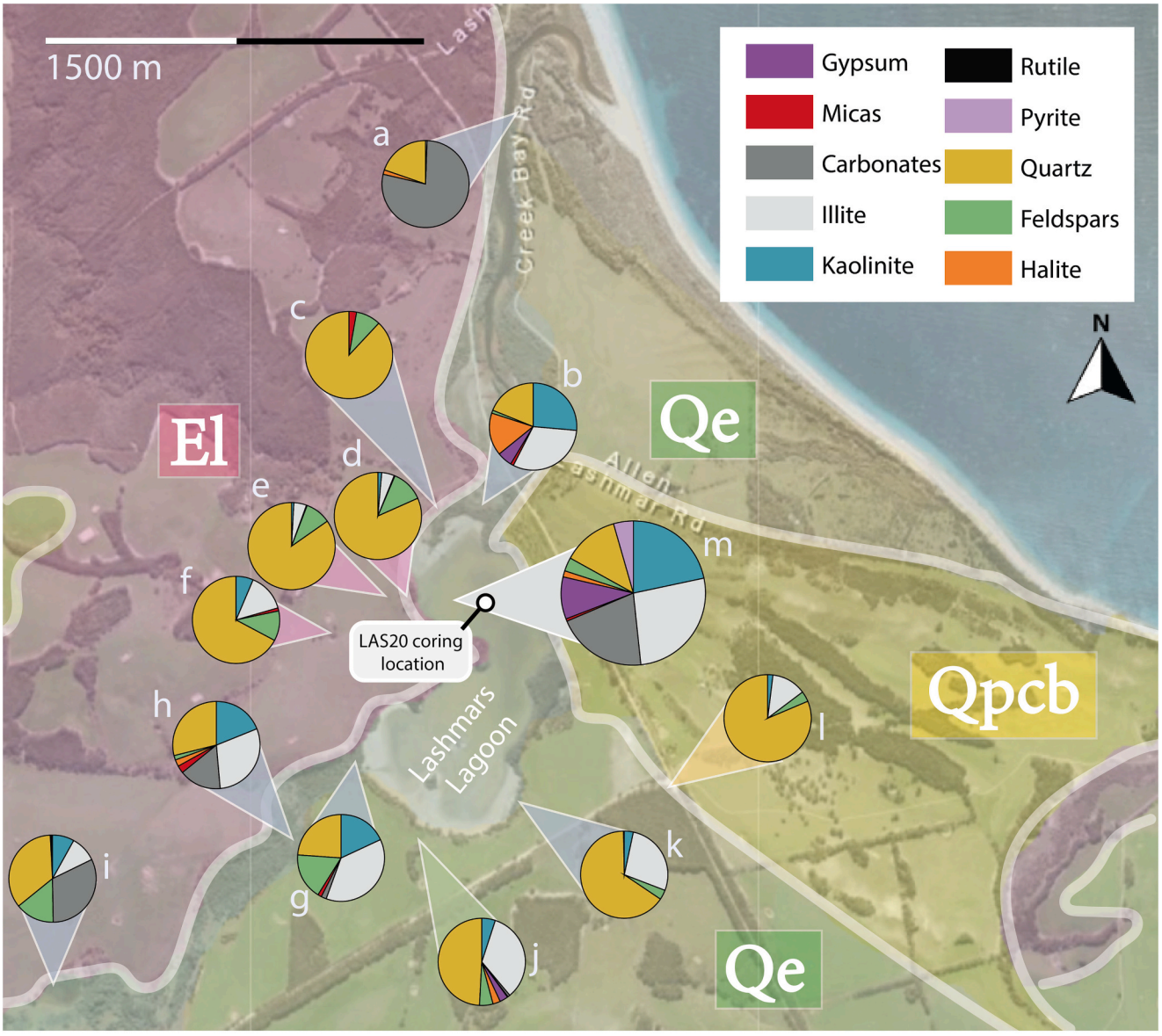

	Sample description	Sample type
a	Chapman River downstream 1	Wet river sediment
b	Chapman River floodplain	Dry floodplain sediment
c	Northwest creek	Wet river sediment
d	Cambrian greywacke, siltstone and shale 1	Catchment soil
e	Cambrian greywacke, siltstone and shale 2	Catchment soil
f	Cambrian greywacke, siltstone and shale 3	Catchment soil
g	Chapman River upstream 1	Wet river sediment
h	Chapman River upstream 2	Wet river sediment
i	Little Lashmars Lagoon	Wet lagoon sediment
j	Quaternary aeolian sands	Catchment soil
k	Southeast winter creekbed	Dry river sediments
l	Quaternary calcreted aeolianite	Catchment soil
m	Lashmars Lagoon surface	Wet lagoon sediment

Fig. 3. Mineralogy of catchment samples and Lashmars Lagoon surface sediments. *Surface geology from* Fig. 1 *is overlayed: pink = Cambrian greywacke, siltstone and shale (El); green = Quaternary aeolian sands (Qe); yellow = Quaternary calcreted aeolianite (Qpcb). The coring location is also denoted in the northern basin of the lake. All four holes in the LAS20 were drilled within the bounds of the circle.* (For interpretation of the references to colour in this figure legend, the reader is referred to the web version of this article.)

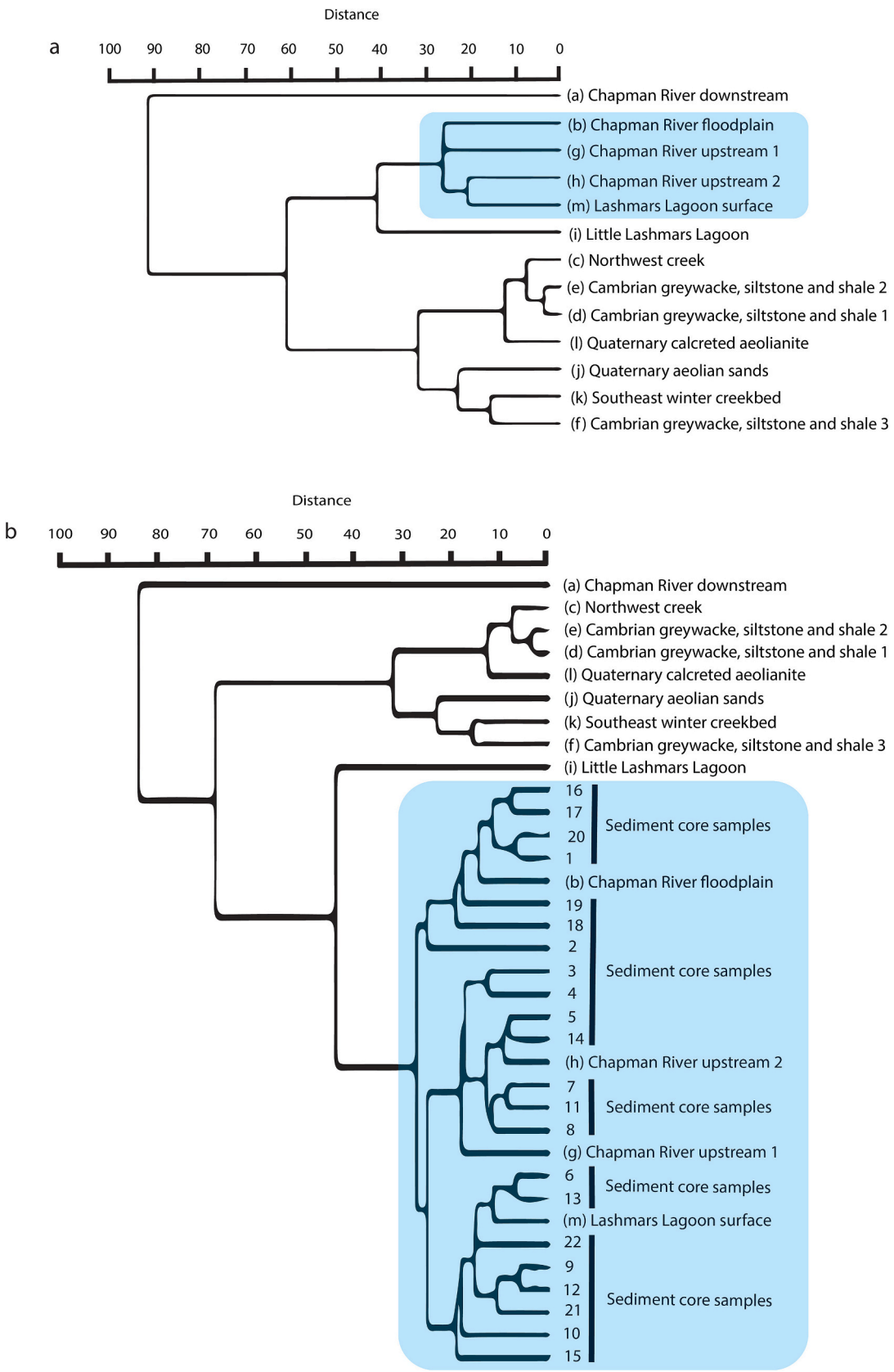

Fig. 4. Classical paired group cluster analysis of (A) catchment soils and sediments and Lashmars Lagoon surface sediments and (B) catchment soils and sediments, and modern (surface) and ancient (sediment core) lake sediments.

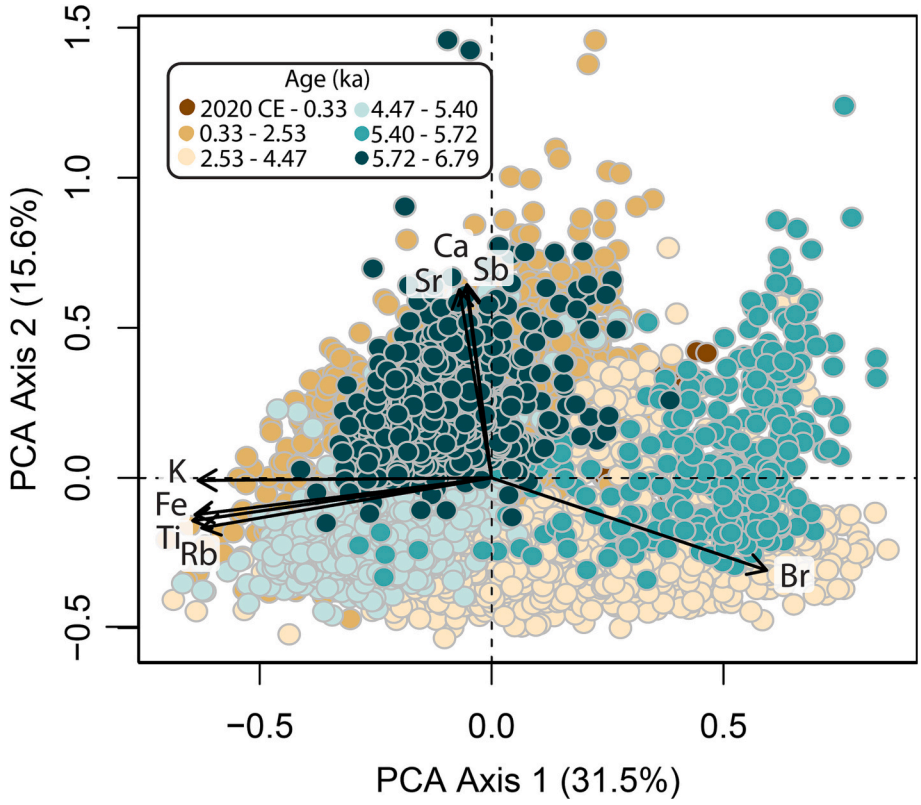

Fig. 5. Principal Components Analysis (PCA) of the filtered XRF elements. *XRF elements strongly correlated with the PCA axis 1 (PC1) and PCA axis 2 (PC2) are displayed. Bromine (Br) is strongly positively correlated with PC1, while the group including potassium (K), iron (Fe), titanium (Ti) and rubidium (Rb) is strongly negatively correlated with PC1. Strontium (Sr), calcium (Ca) and antimony (Sb) are strongly positively correlated with PC2. Points are coloured according to defined stratigraphic units (Table 2). Raw counts for the XRF elements were used.* (For interpretation of the references to colour in this figure legend, the reader is referred to the web version of this article.)

6. Discussion

6.1. Past and present sediment delivery to Lashmars Lagoon

Mineralogical characterisation of catchment soil and inflow and outflow sediments can be used to infer changes in sediment delivery to lakes over time (Morlock et al., 2019). Analysis of catchment and lake surface sediments revealed that the upstream Chapman River sediments clustered with the Lashmars Lagoon surface and deeper core sediments, suggesting that the inflowing Chapman River has been the primary sediment source to Lashmars Lagoon for at least the last ~7000 years (Fig. 4). The Chapman River continues its passage to the sea through an intermittently connected northeast outflow, through which seawater has been known to back up to the lake during storm surges (Clark, 1976). The bulk of the mineralogy in the Chapman River estuary sample was composed of calcite, presumably of biogenic origins as is commonplace in estuarine environments, and it was thus hypothesised that these backwashing events may have been the source of the calcite in Lashmars Lagoon. However, while the floodplain that connects the lake and ocean clustered with the lake sediments and the upstream Chapman River samples, the mineralogy of the downstream Chapman River estuary formed a separate clade to all other samples. This suggests flow between the lake and the sea is either slow or largely absent and thus does not transport much sediment to Lashmars Lagoon. Further, the smaller Little Lashmars Lagoon, upstream on the Chapman River and far from the influence of the sea, had higher concentrations of calcite than Lashmars Lagoon, suggesting that a connection to the sea is not necessary for the presence of calcite in the sediments. This was supported by the presence of intact and presumed in situ calcite bearing organisms including charophyte oospores, foraminifera, and molluscs. However, the transport of calcite from the downstream Chapman River estuary cannot be wholly discounted given the presence of fragmented shells and discrete layers of sandy, shelly, beach-like material in units 5 and 3 that suggest transport into the system from a marine or estuarine source. This is consistent with the identification of uniquely marine molluscs in the lagoon sediments by Clark (1976).

6.2. Interpretation of the geochemical signals in the Lashmars Lagoon sediments

Changes in sediment geochemistry and mineralogy, given careful contextual consideration, can be interpreted in terms of changing climate and catchment processes (Davies et al., 2015). Itrax μXRF core scanning provides detailed assessment of elemental chemical composition, which can be used to infer mineralogy and thus changes in the lake and catchment.

We interpret the Al/K ratio as a weathering proxy at Lashmars Lagoon due to its correlation with the ratio of kaolinite to illite and feldspar ($r = 0.60$, $p = 0.003$; Fig. 6). Chemical weathering tends to be enhanced under relatively warmer and or wetter climates (Francke et al., 2020). In Australia, warmer and wetter climates generally engender increased vegetation, which also enhances weathering via soil-root interactions (Francke et al., 2022). During chemical weathering, chemically labile mineral phases such as feldspar, mica and illite dissolve and are replaced by cation-depleted secondary clays such as kaolinite. In cool and or arid climates, chemical weathering is generally suppressed. Under these conditions, physical weathering predominates and micas are broken down to produce illite, while feldspars are less efficiently converted to kaolinite. Thus, we expect that past periods of higher rainfall and or temperatures (where chemical weathering can be

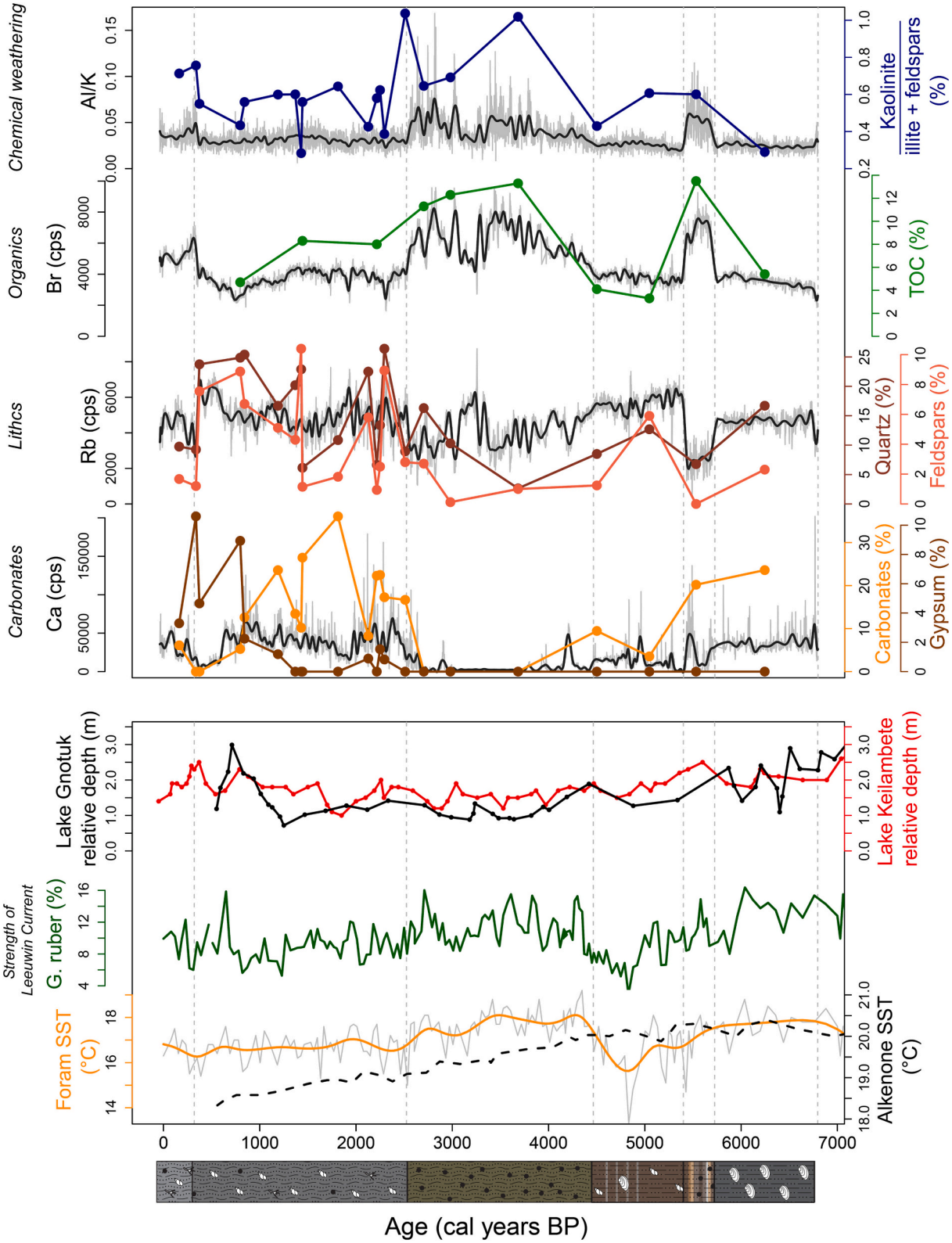

Fig. 6. Summary of the downcore geochemical analyses. ***Top box: geochemical data from Lashmars Lagoon, KI, southern Australia.*** *Left y axes: high resolution (1 mm)* μXRF *elemental scanning of key representive elements and ratios (grey lines with black line showing moving average). Right y axes: calibration of elemental data with organic geochemistry and mineralology (coloured lines with points).* ***Bottom box: comparision to regional palaeoclimate records.*** *Top: relative lake levels from Western Victorian lakes Gnotuk (left y axis) and Lake Keilambete (right y axis) (Wilkins et al., 2013). Middle: abundance of near-surface dweller G. ruber, representative of near-surface stratification changes in sediment core MD03–2611 (offshore KI), a proxy for the strength of the Leeuwin Current (Perner et al., 2018). Bottom: inferred SST from sediment core MD03–2611G (offshore KI) reconstructed from foraminifer data by the modern analogue technique (left y axis) (Barrows et al., 2020) and alkenones (right y axis) (Schneider et al., 2020). All plotted against age (calibrated years BP). Grey vertical dotted lines at stratigraphic boundaries in our Lashmars Lagoon sediment core.*

Table 2
Description of stratigraphic units for the Lashmars Lagoon cores, youngest unit (1) through to oldest unit (6).

Composite depth and age	Visual sediment descriptions and XRF-inferred geochemistry
Unit 1 0–47 cm (2020 CE – 0.33 ka)	***Geochemistry:*** Overall variable geochemistry: high Ca (calcite), at 47 cm abrupt peaks in Br (TOC), S, Fe and pyrite, abrupt drop in K (illite) and pyrite. ***Colour, grain size:*** Mottled dark grey silty clay. ***Composition:*** Highly organic sediments with plant fibres obviously visible, intact and fragmented shells visible throughout. ***Sediment accumulation rate:*** highly variable, very high accumulation rate at the top of the unit
Unit 2 47–319 cm (0.33–2.53 ka)	***Geochemistry:*** High Ca (calcite), low Br (TOC), high K (illite), low Al/K (kaolinite/illite), S intensity highly variable, compared to stable background. ***Colour, grain size:*** Black to very dark grey mottled silty clay, scattered at irregular intervals throughout this section are thin grey horizons, shelly layers, and bands of shiny black very fine clays. ***Composition:*** Clay rich sediments with fragmented and intact shells present throughout, small amounts of fibrous plant material, small twigs and root hairs. ***Sediment accumulation rate:*** relatively high
Unit 3 319–485 cm (2.53–4.47 ka)	***Geochemistry:*** Low Ca (calcite), mostly high Br (TOC), mostly high K (illite), mostly high Al/K (kaolinite/illite). ***Colour, grain size:*** Mottled dark olive silty clay, some darker banding. ***Composition:*** Crumbly, soft, highly organic sediment, very few small shell fragments scattered throughout. ***Sediment accumulation rate:*** relatively low
Unit 4 485–610 cm (4.47–5.40 ka)	***Geochemistry:*** Moderate Ca (calcite), low Br (TOC), very high K (illite), low Al/K (kaolinite/illite). ***Colour, grain size:*** Dark brown to black silty clay with some thin grey horizons. ***Composition:*** Clay rich sediments with fragments of bigger shells scattered throughout, a mostly intact bivalve found near the middle of the unit, some shelly layers. ***Sediment accumulation rate:*** relatively high
Unit 5 610–640 cm (5.40–5.72 ka)	***Geochemistry:*** Variable Ca (calcite), high Br (TOC), low K (illite), high Al/K (kaolinite/illite). ***Colour, grain size:*** Light grey, brown, dark brown and black silty clays. ***Composition:*** Organic rich, crumbly sediments with some shell fragments and fine laminations throughout. ***Sediment accumulation rate:*** relatively low
Unit 6 640–749 cm (5.72–7.01 ka)	***Geochemistry:*** High Ca (statistically linked to calcite), low Br (TOC), high K (illite), low Al/K (kaolinite/illite). ***Colour, grain size:*** Very dark grey silty clay ***Composition:*** Homogenous sediments with large, intact bivalves and smaller fragments scattered throughout. ***Sediment accumulation rate:*** relatively low but variable

increased) would have produced higher relative proportions of kaolinite compared to illite and feldspars, and accordingly higher Al/K ratios. The reverse is assumed for cooler and or more arid climates where chemical weathering is suppressed.

We use Br to infer sediment organic matter content. The C/N ratios (10.79–15.10) and $\delta^{13}C$ values (−21.71 and − 25.44‰) indicated mixed contributions to sediment organic matter from aquatic macrophytes, algae and land plants, albeit weighted towards a predominant algal source (Meyers, 1994). This is also supported by the fact that algae growing in the nutrient limited environments of Australia commonly produce C/N ratios >10 (Cadd et al., 2018; Maxson et al., 2021). We suggest that less saline lagoon conditions and wetter climates would be most conducive to producing high sediment organic matter as these conditions would promote growth of terrestrial plants and are more amenable to aquatic macrophytes and algae productivity.

The group containing K, Ti, Fe and Rb is interpreted to reflect relative detrital input into Lashmars Lagoon. These elements are commonly associated with lithogenic detritus in lake sediments (Davies et al., 2015) and were positively and significantly correlated with the sum of the detrital minerals feldspar, quartz and illite at Lashmars Lagoon (Fig. 6).

We interpret the cluster of elements containing Ca, Sr and Sb to be representative of the combined relative contribution of carbonates (e.g., $CaCO_3$ or $SrCO_3$) and gypsum ($CaSO_4{\cdot}2H_2O$) in the Lashmars Lagoon sediments. Throughout most of the record, this group is predominately a reflection of sediment carbonate content, as gypsum is generally absent or present in very low abundances until after 1 ka (Fig. 6). Carbonate in the Lashmars Lagoon sediment is presumed to be of biogenic origin due to the documented presence of carbonate bearing organisms such as charophyte oospores, foraminifera, and molluscs (Fig. S6). We suggest that increased sediment carbonate reflects periods of higher lake salinity with enhanced concentrations of bioavailable calcium and carbonate ions supporting a diversity of calcium carbonate producing organisms (Battarbee, 2000). Saline lake conditions could be induced by an enhanced hydrological connectivity to the ocean via the Chapman River estuary or by decreased rainfall and increased evaporation in a drier climate. The presence of gypsum requires a high degree of evaporation even with a marine influence (McCaffrey et al., 1987). The presence of gypsum in lake sediments is therefore considered an unequivocal indication of increased evaporation (Burn and Palmer, 2014).

6.3. Climate and catchment variability over the last ~ 7000 years at Lashmars Lagoon

From the geochemical evidence presented in this study, we can make inferences about climate and catchment variability at Lashmars Lagoon over the past 7000 years (Table 2; Fig. 6).

6.3.1. Unit 6 | 7.01–5.72 ka

The geochemistry and sedimentology of unit 6 is unlike any other unit in the core, characterised by the presence of larger intact bivalves, relatively high and stable Ca (carbonates), low Br (organic carbon), and low Al/K (chemical weathering). This combination suggests a more saline lagoon and low chemical weathering of the landscape, potentially linked to drier climates, lower root-soil action or a constant and important marine influence (which may, in itself, be affected by climatic factors). The unresolved potential of these two possible explanations make unequivocal inferences about regional palaeoclimate challenging from geochemical evidence alone.

6.3.2. Unit 5 | 5.72–5.40 ka

Unit 2 is characterised by high Br (organic carbon). This suggests enhanced delivery of allochthonous organic material to the lagoon and or higher autochthonous organic productivity in, a scenario possible with sufficient rainfall to promote vegetation growth in the catchment and to reduce lake water salinity. The abrupt transition at 5.72 ka into this period is striking and may reflect the severance of a more permanent connection to the ocean, e.g., the Chapman River becoming blocked by a beach berm. Interestingly, Ca (carbonate) concentrations throughout this period are variable, potentially explained by the transport of carbonate-rich sediment from the estuary with intermittent marine intrusions, e.g., during storm surges. While the high Al/K ratio suggests accelerated chemical weathering here, this should be interpreted with caution as the ratio of kaolinite to illite and feldspars indicates that chemical weathering remained relatively low. Low chemical weathering might be explained by lower temperatures or reduced soil-root interactions in this period.

6.3.3. Unit 4 | 5.40–4.47 ka

From 5.40 to 4.47 ka there is an extended period of relatively stable geochemistry. Moderate and variable levels of Ca (carbonates) during this time suggest the lagoon was more saline, possibly the result of drier climates and or intermittent marine influence. The sudden transition into this phase at 5.40 ka could suggest the breakdown of the beach berm and the reactivation of the connection of the lagoon to the ocean via the Chapman River estuary. Further evidence for this hypothesis is contained in pronounced sandy and shelly layers throughout this unit which may indicate marine intrusion events. Low Al/K ratios (chemical weathering) may have been caused by lower precipitation, temperature

or root-soil interaction. Low Br (organic carbon) in the lake sediments suggests that productivity in the catchment and lake was low, which is also consistent with lower precipitation.

6.3.4. Unit 3 | 4.47–2.53 ka

The Lashmars Lagoon sediments dated from 4.47 ka – 2.53 ka are generally high in Br (organic carbon), low in Ca (carbonates) and high in Al/K (chemical weathering). This implies that the climate was relatively wet through this period and the connection to the sea largely broken.

6.3.5. Unit 2 | 2.53–0.33 ka

Unit 2 marks the first occurrence of the evaporitic mineral gypsum in the record, clearly defining this period as one of accentuated evaporation and thus an unequivocal drier climate (see section 5.2). This is supported by the other geochemical indices in this phase: we detected very high Ca (carbonates and gypsum), low Br (organic carbon) and a low Al/K (chemical weathering). The existence of bands of shelly, sandy material hints at the possibility of transport of marine or estuarine material from marine intrusions.

6.3.6. Unit 1 | 0.33 ka – 2020 CE

The youngest stratigraphic unit, from 0.33 ka (~1620 CE) to 2020 CE is almost too short to observe long-term trends against background variability. Nevertheless, the increase in Al/K (chemical weathering) and Br (organic carbon) might indicate a recent onset of wetter conditions. However, it is possible that the geochemistry of this period is biased by land use changes associated with colonisation from the early 1800s. Interpreting geochemically inferred climatic and catchment processes in this section of the Lashmars Lagoon record demands contextual considerations beyond the scope of this study.

6.4. Regional climate comparison

Regional records from across southern Australia suggest the climate was relatively wet ~7000 years ago at the onset of the sedimentary sequence at Lashmars Lagoon until ~5.5 ka (De Deckker, 2022; Fletcher and Moreno, 2012; Gouramanis et al., 2013; Wilkins et al., 2013). Lakes Gnotuk and Keilambete in western Victoria, for instance, record inferred lake levels two to three metres higher than present day (Wilkins et al., 2013; Fig. 6). In a synthesis of regional records, De Deckker (2022) defined the Holocene hypsithermal as an unusually warm and wet period from 8.2 to 5.5 ka. In part, this inference is based on a marine sediment core taken offshore KI (MD03–2611G), from which two independent sea surface temperature (SST) proxies record relatively high sea surface temperatures over this period (De Deckker, 2022; Perner et al., 2018; Fig. 6). We expect that warmer ocean conditions would have subsequently led to higher evaporation and local precipitation on KI. In line with this inference, the pollen record from Lashmars Lagoon throughout this period is dominated by Casuarina, and inferred to indicate wetter climates (Clark, 1983a). Overall, the geochemical evidence from Lashmars Lagoon from 7.0 ka to 5.4 ka is more ambiguous, perhaps obscured by local geomorphological idiosyncrasies interfering with a clear climate signal. Interestingly, the beginning of sediment accumulation in Lashmars Lagoon at ~7.0 ka is virtually coincident with the mid-Holocene relative sea-level highstand at ~6.9 ka on the eastern seaboard of Australia (Dougherty et al., 2019). Sea levels then continued to fall through the late Holocene. Given the proximity of Lashmars Lagoon to the sea, it is possible that these earlier sections of the record were influenced disproportionately by a stronger, although abating, marine influence. A diatom record from Lake Alexandrina, a shallow coastal lake on the adjacent mainland, also lends support to this inference as it documents a transition from a marine brackish to oligosaline-freshwater conditions between 7 and 6 ka (Barnett, 1994). The record documents a transition from a marine brackish to oligosaline-freshwater conditions between 7 and 6 ka. Consistent with the diminishing influence of the sea, we do find some geochemical evidence for wetter conditions at Lashmars Lagoon towards the end of the regional hypsithermal from 5.7 to 5.4 ka, in the accumulation of organic carbon from mixed terrestrial and algal sources in the lake. Nonetheless, the interpretation of the climate signal in the sediments of Lashmars Lagoon in this part of the record requires further interrogation through the application of independent palaeoclimate proxies.

Previous studies from eastern Australia suggest a pattern of regional drying starting between 5.5 and 3.3 ka and continuing to the late Holocene (Barr et al., 2019; Donders et al., 2006; Gouramanis et al., 2012; Kemp et al., 2020; Wilkins et al., 2013). For example, lake levels in the western Victorian lakes decline (Kemp et al., 2020; Wilkins et al., 2013) and the alkenone-reconstructed SST record from the core MC03–2611G offshore KI shows a gradual decline after 5.4 ka (De Deckker, 2022; Fig. 6). This roughly aligns with the shift in the pollen record at Lashmars Lagoon from Casuarina to Eucalyptus, reflecting a change from wetter to drier climates around ~5 ka (Clark, 1983a). In line with the drying climate signal, we find circumstantial evidence for a drier period at Lashmars Lagoon from 5.4 to 4.5 ka (inferred saline lake water, low productivity and reduced chemical weathering). However, the climate signal in this period may still be influenced by local geomorphology.

Interestingly, we find evidence for a wetter period from 4.5 to 2.5 ka at Lashmars Lagoon (inferred lower lake water salinity, high productivity in the catchment and lake and enhanced chemical weathering), that does not appear to be reflected in other regional records. However, this period does correspond with a notable increase in the foraminifera *Globigerinoides ruber* in core MC03–2611G from offshore KI (De Deckker, 2022; Perner et al., 2018; Fig. 6). This increase in *G. ruber* abundance was interpreted to reflect an increase in the flow of the Leeuwin Current (LC) around the southern coast of Australia. Today the Leeuwin Current, which is at its strongest in autumn and winter, transports warm, low-saline water from the tropics across the southern coast of Australia (Godfrey and Ridgway, 1985). This, in turn, could then lead to an increase in locally derived sea surface evaporation and subsequent precipitation on land. Foraminifera-based reconstruction of SST suggest increased SST around 4.5–2.5 ka, at least in the autumn and winter months where the influence of the LC is strongest. However, the foraminifera-based SST reconstruction contrasts with the alkenone (Uk'_{37}) SST reconstruction from the same core material which suggests a progressive decrease in SST from 7.4 ka until present (Perner et al., 2018; Fig. 6). These differences may relate to different seasonal biases in the temperature proxies, or other uncertainties with one of the two methods. Despite these uncertainties, it appears that changes in the ocean circulation around southern Australia may have countered the trend towards drying climate in eastern Australia after ~4.5 ka, with the result that Lashmars Lagoon experienced relatively wet conditions through to ~2.5 ka.

Broadly speaking, our record at Lashmars Lagoon shows convincing evidence of increasingly dry conditions throughout the Late Holocene from ~2.5 ka (e.g., the first occurrence and increase of the evaporite gypsum). The continual decline of SST recorded in the nearby offshore marine sediment core MC03–2611G from about ~2.5 ka until present day may provide a possible mechanism to explain decreased precipitation on KI (De Deckker, 2022). Further, the timing of the shift to drier climates at Lashmars Lagoon at ~2.5 ka coincides with the previously recorded increase in microcharcoal (Clark, 1983a) and a radiocarbon-dated lake desiccation horizon from the nearby Coorong (Ahmad, 1996). The shift also roughly correlates with an increase in diatom-inferred salinity from an undated sedimentary record from Lashmars Lagoon (Illman, 1998). Previous studies from eastern mainland Australia, as well as Tasmania, have suggested that the Late Holocene was associated with an intensification of ENSO-like variability and increased El Niño-like states (Barr et al., 2019; Perner et al., 2018). Several of these records document the Late Holocene drying after 3.5 ka (Fletcher and Moreno, 2012; Gouramanis et al., 2013; Gouramanis et al., 2012; Wilkins et al., 2013). However, the Lashmars Lagoon record suggests that the climate and environmental conditions on KI did not

deteriorate sufficiently to cause a significant shift in the geochemistry until 2.5 ka, up to 1000 years later than sites further to the east. We suggest that the continued, albeit weakening, supply of warmer tropical water in autumn and winter from the LC, buffered KI against the regionally observed late Holocene shift to a drier climate.

6.5. Future directions

Our high-resolution record provides the framework for more detailed palaeoenvironmental reconstructions on KI using a wider array of proxies. Palaeoecological and palaeofire reconstructions using pollen, sedimentary ancient DNA and charcoal are underway, and promise to help resolve remaining uncertainties in the geochemical record presented here, providing a more robust record of climatic and environmental evolution in the region. Future work should also focus on building a better understanding of the history of Aboriginal peoples on the island, from both scientific and First Nations' knowledge systems perspectives, necessary for holistic understanding of Earth system dynamics over the past ~7000 years in southern Australia.

7. Conclusions

In summary, we interpret the changes in sediment geochemistry over the past 7000 years at Lashmars Lagoon, Kangaroo Island (Karti/Karta), to represent changes in climate overprinted by shifts in local coastal geomorphology and sea level. Overall, our record is generally cohesive with regional paleoclimate reconstructions that suggest a general pattern of drying into the late Holocene. However, geochemical evidence from Lashmars Lagoon suggests a distinctive wet period from 4.5 to 2.5 ka not recorded in other palaeoclimate reconstructions from southeastern Australia. Importantly, we find evidence to suggest that precipitation on Kangaroo Island (Karti/Karta) may be linked to fluctuations in the strength of the Leeuwin Current (LC) which transports warm tropical water down the western Australian coast to Kangaroo Island (Karti/Karta) in autumn and winter and is linked to changes in variability of the El Niño Southern Oscillation (ENSO).

Author contributions

LD worked on the study design, undertook field and lab work, data analysis and interpretation, and wrote the first draft of the manuscript; JT, WL, AF, CM assisted with field work; JT, HC, AF and LJ-M helped with the study design and interpretation; LJ-M processed the organic geochemistry and some of the XRD samples with the assistance of PAH; SL helped with interpretation; WL made Fig. 1; CM, AZ, GJ, PG, DC, ZT contributed to lab work, data analysis and interpretation of the chronology; all authors contributed to the editing of the manuscript.

Funding information

This work was supported by the Australian Nuclear Science and Technology Organisation (ANSTO) through ANSTO Portal Grants (AP12819, AP13336, AP13662) and an AINSE Ltd. Postgraduate Research Award. We acknowledge the financial support for the Centre for Accelerator Science, at ANSTO, through the Australian National Collaborative Research Infrastructure Strategy (NCRIS). Pollen dates were supported in part by an internship award through the Australasian Quaternary Association (AQUA), Centre of Excellence for Australian Biodiversity and Heritage (CABAH) and the Chronos ^{14}Carbon-Cycle Facility at the University of New South Wales. Field work was supported by the Environment Institute, The University of Adelaide, and Sealink. LD was supported by an Australian Government Research Training Program Scholarship and by a Cadetship from the ARC Centre of Excellence for Australian Biodiversity and Heritage (CABAH).

CRediT authorship contribution statement

Lucinda Cameron Duxbury: Conceptualization, Formal analysis, Funding acquisition, Investigation, Methodology, Visualization, Writing – original draft. **Lluka Yohanni Johns-Mead:** Conceptualization, Formal analysis, Investigation, Methodology, Writing – review & editing. **Haidee Cadd:** Conceptualization, Formal analysis, Funding acquisition, Investigation, Methodology, Supervision, Writing – review & editing. **Alexander Francke:** Conceptualization, Formal analysis, Funding acquisition, Investigation, Methodology, Writing – review & editing. **Stefan C. Löhr:** Formal analysis, Investigation, Methodology, Writing – review & editing. **Wallace Boone Law:** Investigation, Methodology, Resources, Visualization, Writing – review & editing. **Linda Armbrecht:** Conceptualization, Supervision, Writing – review & editing. **Philip Anthony Hall:** Methodology, Resources, Validation. **Atun Zawadzki:** Formal analysis, Investigation, Resources, Writing – review & editing. **Geraldine E. Jacobsen:** Investigation, Methodology, Resources, Writing – review & editing. **Patricia S. Gadd:** Investigation, Methodology, Resources. **David P. Child:** Methodology, Resources, Validation. **Charles Maxson:** Methodology, Writing – review & editing. **Zoë Amber Thomas:** Resources. **Jonathan James Tyler:** Conceptualization, Formal analysis, Funding acquisition, Investigation, Methodology, Resources, Supervision, Validation, Visualization, Writing – review & editing.

Declaration of Competing Interest

The authors declare that they have no known competing financial interests or personal relationships that could have appeared to influence the work reported in this paper.

Data availability

The data presented in this study will available on the online soon in PANGAEA database.

Duxbury, Lucinda; Johns-Mead, Lluka Yohanni; Cadd, Haidee; Francke, Alexander; Löhr, Stefan; Law, W. Boone; Armbrecht, Linda; Hall, P. Anthony; Zawadzki, Atun; Jacobsen, Geraldine; Gadd, Patricia; Child, David; Maxson, Charles; Thomas, Zoë; Tyler, Jonathan: Chronology, μXRF, XRD and organic geochemistry from a lake sediment core from Lashmars Lagoon, Kangaroo Island (Karti/Karta), southern Australia, for the last 7 kyr. PANGAEA, [doi] (dataset in review).

Duxbury, Lucinda; Johns-Mead, Lluka; Löhr, Stefan; Hall, P. Anthony; Francke, Alexander; Maxson, Charles; Law, W. Boone; Tyler, Jonathan: Mineralogical characterisation from XRD analysis of sediments and soils in the catchment of Lashmars Lagoon, Kangaroo Island (Karti/Karta), southern Australia. PANGAEA, [doi] (dataset in review).

Acknowledgements

In Australia, we work and live on Aboriginal land. We pay our respects to elders past, present, and emerging and acknowledge that sovereignty was never ceded. This research was developed and conducted on Kaurna Yerta (Kaurna land) at The University of Adelaide and on Karti/Karta (Kangaroo Island), a place of deep cultural and spiritual significance for Aboriginal people in South Australia, as well as for the Tasmanian Aboriginal women and their descendants who were brought to the island in the early days of European invasion. Some notes on the pronunciation of *Karti/Karta*:

'K' is pronounced halfway between the English 'k' and 'g'.

'a' is as in the English words: mama, papa, visa

'rt' is one sound which involves curling your tongue back in your mouth while pronouncing an English 't' – similar to the 'rt' in cart with a strong North American accent

'i' as in the English words: bit, pit, sit or 'a' as in the English word 'delta'.

We recommend that readers consult with Ngarrindjeri and Kaurna speakers and Elders to practise pronunciation and note that the language remains the intellectual property of the respective communities.

Thanks to Jack Duxbury, Tristan Fenn, John Tibby, Fletcher Nixon, Lucy Stokes, Amelia Orchard, Lucy Duldig and Eleanor McCall for help with field work and to Bronwyn Cooter and the Lashmar family for providing site access and sharing their knowledge with us. Thanks as well to all the professional staff at the Australian Nuclear Science and Technology Organisation (ANSTO). Conversations with Darren Ray and Germain Bayon were critical for the development of ideas. Benjamin Wade from Adelaide Microscopy ran samples to help verify the presence of in-situ gypsum.

The authors would like to thank an anonymous reviewer and the editor Howard Falcon-Lang for their helpful suggestions to improve the quality of this manuscript.

Appendix A. Supplementary data

Supplementary data to this article can be found online at https://doi.org/10.1016/j.palaeo.2023.111928.

References

Ahmad, R., 1996. Late Holocene major Australian arid period revealed by direct sedimentological evidence from lakes in the Coorong region of South Australia. Geology 24, 619–622.

Amery, R., Greenwood, S., Morley, J., 2021. Kaurna warrapiipa = Kaurna dictionary : Kaurna to English, English to Kaurna. Published by Kaurna Warra Pintyanthi in association with Discipline of Linguistics, School of Humanities, the Univeristy of Adelaide, Adelaide.

Aquino-López, M.A., Blaauw, M., Christen, J.A., Sanderson, N.K., 2018. Bayesian Analysis of Pb-210 Dating. J. Agric. Biol. Environ. Stat. 23, 317–333.

Barnett, E.J., 1994. A Holocene paleoenvironmental history of Lake Alexandrina, South Australia. J. Paleolimnol. 12, 259–268.

Barr, C., Tibby, J., Leng, M., Tyler, J., Henderson, A., Overpeck, J., Simpson, G., Cole, J., Phipps, S., Marshall, J., 2019. Holocene el Niño–southern Oscillation variability reflected in subtropical Australian precipitation. Sci. Rep. 9, 1–9.

Barrows, T., Perner, K., De Deckker, P., 2020. Sea surface temperature from sediment cores MD03–2611G and MUC-3 reconstructed by modern analogue technique. PANGAEA, https://doi.org/10.1594/PANGAEA.911822, De Deckker, P., Moros, M., Blanz, T., Schneider, R., Barrows, T., Perner, K., Multidataset for sediment cores MD03-2611 and SS0206-GC15 taken offshore southern Australia. PANGAEA, doi: 10.1594/PANGAEA.911846.

Battarbee, R.W., 2000. Palaeolimnological approaches to climate change, with special regard to the biological record. Quat. Sci. Rev. 19, 107–124.

Belperio, A., Flint, R., 1999. Geomorphology and geology. A Biological survey of Kangaroo Island, South Australia. In: Robinson, A.C., Armstrong, D.M. (Eds.), A Biological Survey of Kangaroo Island, South Australia, 1989 & 1990, Heritage and Biodiversity Section. Department for Environment, Heritage and Aboriginal Affairs, South Australia, pp. 19–32.

Binskin, M., Bennett, A., Macintosh, A., 2020. Royal Commission into National Natural Disaster Arrangements Report. Commonwealth of Australia, Canberra.

Blaauw, M., Christen, J.A., 2011. Flexible paleoclimate age-depth models using an autoregressive gamma process. Bayesian Anal. 6 (3), 457–474.

Bond, N.R., Lake, P.S., Arthington, A.H., 2008. The impacts of drought on freshwater ecosystems: an Australian perspective. Hydrobiologia 600, 3–16.

Bowman, D.M., 1998. The impact of Aboriginal landscape burning on the Australian biota. New Phytol. 140, 385–410.

Bureau of Meteorology, 2020. State of the Climate 2020. Commonwealth Scientific and Industrial Research Organisation (CSIRO), Australia.

Bureau of Meteorology, 2023. Climate data online. Melbourne: Commonwealth of Australia, Bureau of Meteorology. Available from. http://www.bom.gov.au/climate/data/?ref=ftr [Accessed 11th August 2023].

Bureau of Meteorology, A, 2022. Australian climate influences. Available from. http://www.bom.gov.au/watl/about-weather-and-climate/australian-climate-influences.shtml [Accessed 12th August 2023].

Burn, M.J., Palmer, S.E., 2014. Solar forcing of Caribbean drought events during the last millennium. J. Quat. Sci. 29, 827–836.

Burnett, A.P., Soreghan, M.J., Scholz, C.A., Brown, E.T., 2011. Tropical East African climate change and its relation to global climate: a record from Lake Tanganyika, Tropical East Africa, over the past 90+ kyr. Palaeogeogr. Palaeoclimatol. Palaeoecol. 303, 155–167.

Cadd, H.R., Tibby, J., Barr, C., Tyler, J., Unger, L., Leng, M.J., Marshall, J.C., McGregor, G., Lewis, R., Arnold, L.J., 2018. Development of a southern hemisphere subtropical wetland (Welsby Lagoon, south-East Queensland, Australia) through the last glacial cycle. Quat. Sci. Rev. 202, 53–65.

Cadd, H., Sherborne-Higgins, B., Becerra-Valdivia, L., Tibby, J., Barr, C., Forbes, M., Cohen, T.J., Tyler, J., Vandergoes, M., Francke, A., 2022. The application of pollen radiocarbon dating and bayesian age-depth modeling for developing robust geochronological frameworks of wetland archives. Radiocarbon 64, 213–235.

Clark, R.L., 1976. Vegetation History and the Influence of the Sea at Lashmar's Lagoon, Kangaroo Island, South Australia, 3,000 BP to the Present Day. Monash University.

Clark, R.L., 1983a. Fire History from Fossil Charcoal in Lake and Swamp Sediments. Australian National University.

Clark, R.L., 1983b. Pollen and charcoal evidence for the effects of Aboriginal burning on the vegetation of Australia. Archaeol. Ocean. 18, 32–37.

Davey, S.M., Sarre, A., 2020. Editorial: the 2019/20 Black Summer bushfires. Aust. For. 83 (2), 47–51.

Davies, S., Lamb, H., Roberts, S., 2015. Micro-XRF core scanning in palaeolimnology: recent developments. In: Croudace, I., Rothwell, R. (Eds.), Micro-XRF Studies of Sediment Cores. Developments in Paleoenvironmental Research 17.

De Deckker, P., 2022. The Holocene hypsithermal in the Australian region. Quater Sci Adva 7, 100061.

Dodson, J., 2001. Holocene vegetation change in the mediterranean-type climate regions of Australia. The Holocene 11, 673–680.

Donders, T.H., Wagner, F., Visscher, H., 2006. Late Pleistocene and Holocene subtropical vegetation dynamics recorded in perched lake deposits on Fraser Island, Queensland, Australia. Palaeogeogr. Palaeoclimatol. Palaeoecol. 241, 417–439.

Dougherty, A.J., Thomas, Z.A., Fogwill, C., Hogg, A., Palmer, J., Rainsley, E., Williams, A.N., Ulm, S., Rogers, K., Jones, B.G., 2019. Redating the earliest evidence of the mid-Holocene relative sea-level highstand in Australia and implications for global sea-level rise. PLoS One 14, e0218430.

Environmental Protection Agency, 2013. Kangaroo Island NRM Regional Summary 2013 Aquatic Ecosystem Condition Report. Available from. https://www.epa.sa.gov.au/reports_water/ki_creeks-ecosystem-2013 [Accessed: 12th August 2023].

Feng, M., Meyers, G., Pearce, A., Wijffels, S., 2003. Annual and interannual variations of the Leeuwin current at 32 S. J. Geophys. Res. Oceans 108.

Flannery, T.F., 1990. Pleistocene Faunal loss: Implications of the Aftershock for Australia's past and Future. Archaeol. Ocean. 25, 45–55.

Fletcher, M.-S., Moreno, P.I., 2012. Have the Southern Westerlies changed in a zonally symmetric manner over the last 14,000 years? A hemisphere-wide take on a controversial problem. Quat. Int. 253, 32–46.

Francke, A., Conze, R., Pierdominici, S., Gorgas, T., 2017. Core Correlation using Corelyzer, Corelator and the Drilling Information System. In: Harms, U. (Ed.), Planning, Managing, and Executing Continental Scientific Drilling Projects, 3rd Ed. GFZ German Research Centre for Geosciences, Potsdam, pp. 93–101.

Francke, A., Holtvoeth, J., Codilean, A.T., Lacey, J.H., Bayon, G., Dosseto, A., 2020. Geochemical methods to infer landscape response to Quaternary climate change and land use in depositional archives: a review. Earth Sci. Rev. 207, 103218.

Francke, A., Dosseto, A., Forbes, M., Cadd, H., Short, J., Sherborne-Higgins, B., Constantine, M., Tyler, J., Tibby, J., Marx, S.K., 2022. Catchment vegetation and erosion controlled soil carbon cycling in South-Eastern Australia during the last two glacial-interglacial cycles. Glob. Planet. Chang. 217, 103922.

Gale, M.-A., 2009. Ngarrindjeri Elders and Community. Ngarrindjeri Dictionary. David Uniapon College of Indigenous Education and Research, Wingfield.

Gammage, B., 2013. The Biggest Estate on Earth: How Aborigines Made Australia. Allen & Unwin, Crows Nest, New South Wales.

Gillett, N., Kell, T., Jones, P., 2006. Regional climate impacts of the Southern Annular Mode. Geophys. Res. Lett. 33.

Godfrey, J., Ridgway, K., 1985. The large-scale environment of the poleward-flowing Leeuwin current, Western Australia: longshore steric height gradients, wind stresses and geostrophic flow. J. Phys. Oceanogr. 15, 481–495.

Gouramanis, C., Dodson, J., Wilkins, D., De Deckker, P., Chase, B., 2012. Holocene palaeoclimate and sea level fluctuation recorded from the coastal Barker Swamp, Rottnest Island, South-western Western Australia. Quat. Sci. Rev. 54, 40–57.

Gouramanis, C., De Deckker, P., Switzer, A.D., Wilkins, D., 2013. Cross-continent comparison of high-resolution Holocene climate records from southern Australia—Deciphering the impacts of far-field teleconnections. Earth Sci. Rev. 121, 55–72.

Hammer, O., Harper, D., Ryan, R., 2001. PAST: Paleontological statistics software package for education and data analysis. Palaeontol. Electron. 4, 9.

Head, L., 1989. Prehistoric Aboriginal impacts on Australian vegetation: an assessment of the evidence. Austr. Geograph. 20, 37–46.

Hennessy, K., Lawrence, J., Mackey, B., 2022. IPCC sixth assessment report (AR6): climate change 2022-impacts, adaptation and vulnerability: regional factsheet Australasia. Available from. https://www.ipcc.ch/report/ar6/wg2/about/factsheets [Accessed 12th August 2023].

Heyng, A.M., Mayr, C., Lücke, A., Striewski, B., Wastegård, S., Wissel, H., 2012. Environmental changes in northern New Zealand since the Middle Holocene inferred from stable isotope records (δ15N, δ13C) of Lake Pupuke. J. Paleolimnol. 48, 351–366.

Hogg, A.G., Heaton, T.J., Hua, Q., Palmer, J.G., Turney, C.S., Southon, J., Bayliss, A., Blackwell, P.G., Boswijk, G., Ramsey, C.B., 2020. SHCal20 Southern Hemisphere calibration, 0–55,000 years cal BP. Radiocarbon 62, 759–778.

Horton, D., 1982. The burning question: Aborigines, fire and Australian ecosystems. Mankind 13, 237–252.

Hotchkis, M.A.C., Child, D.P., Froehlich, M.B., Wallner, A., Wilcken, K., Williams, M., 2019. Actinides AMS on the VEGA accelerator. Nucl. Instrum. Methods Phys. Res., Sect. B 438, 70–76.

Hua, Q., Jacobsen, G.E., Zoppi, U., Lawson, E.M., Williams, A.A., Smith, A.M., McGann, M.J., 2001. Progress in radiocarbon target preparation at the ANTARES AMS Centre. Radiocarbon 43, 275–282.

Illman, M., 1998. Reconstruction of the late holocene palaeosalinity and palaeoecology of Lashmar's Lagoon, Kangaroo Island, South Australia. In: Proceedings : the first

Australian Diatom Workshop, Deakin University. Warrnambool Campus, Warrnambool, Australia, pp. 41–51, 1-3 February 1997 1.
Kemp, C., Tibby, J., Arnold, L., Barr, C., Gadd, P., Marshall, J., Mcgregor, G., Jacobsen, G., 2020. Climates of the last three interglacials in subtropical eastern Australia inferred from wetland sediment geochemistry. Palaeogeogr. Palaeoclimatol. Palaeoecol. 538, 109463.
Kershaw, A., D'Costa, D., Mason, J.M., Wagstaff, B., 1991. Palynological evidence for Quaternary vegetation and environments of mainland southeastern Australia. Quat. Sci. Rev. 10, 391–404.
Kershaw, A.P., Clark, J.S., Gill, A.M., D'Costa, D.M., 2002. A history of fire in Australia. Flamm. Austr. 1, 3–25.
Kohen, J.L., 1995. Aboriginal Environmental Impacts. UNSW Press, Sydney.
Lampert, R.J., 1981. The great Kartan mystery. Aust. Archaeol. 12 (1), 107–109.
Maxson, C., Tibby, J., Marshall, J., Kent, M., Tyler, J., Barr, C., McGregor, G., Cadd, H., Schulz, C., Lomax, B.H., 2021. Fourier transform infrared spectroscopy as a tracer of organic matter sources in lake sediments. Palaeogeogr. Palaeoclimatol. Palaeoecol. 581, 110622.
McCaffrey, M., Lazar, B., Holland, H., 1987. The evaporation path of seawater and the coprecipitation of Br (super-) and K (super+) with halite. J. Sediment. Res. 57, 928–937.
Meyers, P.A., 1994. Preservation of elemental and isotopic source identification of sedimentary organic matter. Chem. Geol. 114, 289–302.
Meyers, P.A., Lallier-Vergès, E., 1999. Lacustrine sedimentary organic matter records of late Quaternary paleoclimates. J. Paleolimnol. 21, 345–372.
Middleton, J.F., Bye, J.A., 2007. A review of the shelf-slope circulation along Australia's southern shelves: Cape Leeuwin to Portland. Prog. Oceanogr. 75, 1–41.
Morlock, M.A., Vogel, H., Nigg, V., Ordoñez, L., Hasberg, A.K., Melles, M., Russell, J.M., Bijaksana, S., 2019. Climatic and tectonic controls on source-to-sink processes in the tropical, ultramafic catchment of Lake Towuti, Indonesia. J. Paleolimnol. 61, 279–295.
Parnell, A., 2014. Bchron: Radiocarbon dating, age-depth modelling, relative sea level rate estimation, and non-parametric phase modelling. R package version 4.
Perner, K., Moros, M., De Deckker, P., Blanz, T., Wacker, L., Telford, R., Siegel, H., Schneider, R., Jansen, E., 2018. Heat export from the tropics drives mid to late Holocene palaeoceanographic changes offshore southern Australia. Quat. Sci. Rev. 180, 96–110.
R Core Team, 2022. R: A language and environment for statistical computing. R Foundation for Statistical Computing, Vienna, Austria. Available from. https://www.R-project.org/ [Accessed 1st April 2022].
Renberg, I., Hansson, H., 2008. The HTH sediment corer. J. Paleolimnol. 40, 655–659.
Robinson, A., Armstrong, D., 1999. A Biological Survey of Kangaroo Island South Australia, 1989 and 1990. In: Heritage and Biodiversity Section. Department for Environment, Heritage and Aboriginal Affairs, South Australia.
Schneider, R., Blanz, T., De Deckker, P., 2020. Alkenones in sediment core MD03–2611G. In: PANGAEA. https://doi.org/10.1594/PANGAEA.911840. De Deckker, P., Moros, M., Blanz, T., Schneider, R., Barrows, T., Perner, K., 2020. Multidataset for sediment cores MD03-2611 and SS0206-GC15 taken offshore southern Australia. PANGAEA, doi:10.1594/PANGAEA.911846.
Seki, A., Tada, R., Kurokawa, S., Murayama, M., 2019. High-resolution Quaternary record of marine organic carbon content in the hemipelagic sediments of the Japan Sea from bromine counts measured by XRF core scanner. Prog Earth Planet Sci 6, 1–12.
Sheng, Y., Xu, X., 2019. The productivity impact of climate change: evidence from Australia's Millennium drought. Econ. Model. 76, 182–191.
Shulmeister, J., Goodwin, I., Renwick, J., Harle, K., Armand, L., McGlone, M., Cook, E., Dodson, J., Hesse, P., Mayewski, P., 2004. The Southern Hemisphere westerlies in the Australasian sector over the last glacial cycle: a synthesis. Quat. Int. 118, 23–53.
Singh, G., Kershaw, A.P., Clark, R., 1981. Quaternary vegetation and fire history in Australia. Fire Austr. Biota 23–54.
Taylor, R., 2008. Unearthed: The Aboriginal Tasmanians of Kangaroo Island. Wakefield Press, Kent Town.
Turney, C., Becerra-Valdivia, L., Sookdeo, A., Thomas, Z.A., Palmer, J., Haines, H.A., Cadd, H., Wacker, L., Baker, A., Andersen, M.S., 2021. Radiocarbon protocols and first intercomparison results from the Chronos ^{14}Carbon-Cycle Facility, University of New South Wales, Sydney, Australia. Radiocarbon 63, 1003–1023.
Van Dijk, A.I., Beck, H.E., Crosbie, R.S., De Jeu, R.A., Liu, Y.Y., Podger, G.M., Timbal, B., Viney, N.R., 2013. The Millennium Drought in Southeast Australia (2001–2009): Natural and human causes and implications for water resources, ecosystems, economy, and society. Water Resour. Res. 49, 1040–1057.
Wacker, L., Bonani, G., Friedrich, M., Hajdas, I., Kromer, B., Němec, M., Ruff, M., Suter, M., Synal, H.-A., Vockenhuber, C., 2010. MICADAS: routine and high-precision radiocarbon dating. Radiocarbon 52, 252–262.
Wei, G., Li, X.H., Liu, Y., Shao, L., Liang, X., 2006. Geochemical record of chemical weathering and monsoon climate change since the early Miocene in the South China Sea. Paleoceanography 21.
Wilcken, K.M., Hotchkis, M., Levchenko, V., Fink, D., Hauser, T., Kitchen, R., 2015. From carbon to actinides: a new universal 1MV accelerator mass spectrometer at ANSTO. Nucl. Instrum. Methods Phys. Res., Sect. B 361, 133–138.
Wilkins, D., Gouramanis, C., De Deckker, P., Fifield, L.K., Olley, J., 2013. Holocene lake-level fluctuations in Lakes Keilambete and Gnotuk, southwestern Victoria, Australia. The Holocene 23, 784–795.
Wright, H.E., 1967. A square-rod piston sampler for lake sediments. J. Sediment. Res. 37, 975–976.
Ziegler, M., Jilbert, T., de Lange, G.J., Lourens, L.J., Reichart, G.J., 2008. Bromine counts from XRF scanning as an estimate of the marine organic carbon content of sediment cores. Geochem. Geophys. Geosyst. 9.